Development and Thermo-mechanical Reliability Assessment of Fiber Reinforced Polymers in Lightweight PV Modules towards Vehicle-integrated Photovoltaics

Bin Luo [1,2,3,4*], Jonathan Govaerts [2,3,4], Rik Van Dyck [1,2,3,4], Tom Borgers [2,3,4], Bart Ruttens [5], Marta Casasola Paesa [2,3,4], Jan D'Haen [3], Loic Tous [2,3,4], Hariharsudan Sivaramakrishnan Radhakrishnan [2,3,4], Michael Daenen [2,3,4], Aart Willem Van Vuure [1], Jef Poortmans [1,2,3,4]

[1]KU Leuven, Oude Markt 13, 3000 Leuven, Belgium

[2]Imec, imo-imomec, Thor Park 8320, 3600 Genk, Belgium

[3]Hasselt University, imo-imomec, Martelarenlaan 42, 3500 Hasselt, Belgium

[4]EnergyVille, imo-imomec, Thor Park 8320, 3600 Genk, Belgium

[5]Imec, imomec, Wetenschapspark 1, 3590 Diepenbeek, Belgium

[*]Corresponding author: Bin Luo, bin.luo@imec.be

Abstract

Weight reduction by omitting the use of bulky glass in c-Si photovoltaic (PV) modules is an important consideration of module development for vehicle-integrated photovoltaics (VIPV). Various approaches to achieve lightweight modules are proposed, yet there are many concerns regarding the reliability of such modules compared to standard glass-glass or glass-backsheet configurations. In this work, we investigate the thermo-mechanical behavior of LW modules with a multiwire design specifically aiming to VIPV applications. The developed modules consist of a commercially available carbon-fiber reinforced polypropylene backsheet and are compared to glass-fiber reinforced polypropylene backsheet modules. To enhance the thermomechanical reliability, polymer encapsulant and interconnection foil are substituted by glass-fiber reinforced composite encapsulant with the carbon-fiber reinforced polypropylene backsheet, thereby leading to ~ 2.9 % fill factor (FF) decrease with a limited degradation after 200 thermal cycles. A failure mechanism analysis using electroluminescence and X-ray-based micro-tomography is carried out after thermal cycling tests, clearly demonstrating that thermal stresses introduce deformation of wire interconnects. A modified high-temperature thermal cycling test (- 40 to 110 °C, 3.5 hours) is implemented to observe the fast degradation of interconnects in compliance with VIPV conditions. The resulting fatigue stresses account for wire breakage in-between cells in the glass-fiber reinforced polypropylene module, while this effect is less pronounced in the carbon-fiber reinforced polypropylene backsheet module, indicating better thermomechanical reliability of the carbon-fiber reinforced polypropylene backsheet module. Herein, the current results could provide guidelines for lightweight PV module design (with a weight of 4.8 kg/m^2) in the thermomechanical aspect. This research sheds light on the potential of lightweight modules specifically for VIPV applications.

Keywords: Vehicle-integrated Photovoltaics, lightweight PV modules, glass-fiber reinforced polymer, carbon-fiber reinforced polymer, reliability

I. INTRODUCTION

The share of electric vehicles (EV) in the overall car market has constantly been rising in recent years [1, 2]. VIPV allows charging EVs during daytime and off-grid; therefore, the produced electricity can be used to extend the driving range of EVs and reduce the amount of charging stations/times.

Many researchers have developed comprehensive simulation studies concerning the accessibility, significance, and profitability of VIPV concepts [3-8]. In practice, being different from traditional terrestrial PV modules, VIPV modules require customization to cover the majority of available space (roof, body panels, etc.), high efficiency due to the limited available space, outstanding aesthetics to attract customers and ultra-lightweight to maximize range [9]. Currently, a majority of VIPV products target panoramic PV roofs, composed of glasses as both front and back cover, with a mass of more than 15 kg/m^2 [10]. In this case, the additional weight to integrate PV is relatively low, being only the weight of the strings. Given that energy yield provided by a solar roof is normally limited using a commercial Si-solar module (within a few hundred-Watt peak power output), it is significant to widely apply PV onto the rest of the vehicle's body (e.g., hood or door) to reach a higher integration level [3]. However, the glass-glass structure is not suited in this regard, as the massive use of glasses would significantly increase the weight of the vehicle and raise safety concerns. Although novel lightweight (LW) PV modules have already been proposed for other applications (less than 6 kg/m^2) [10-12], e.g., honeycomb modules for building-integrated photovoltaics (BIPV) applications [10,11,13], materials employed in VIPV should be selected scrupulously in order to fulfill the various safety requirements and standards for both PV and automotive [14-16].

Inspired by the LW materials that have been used in the automotive field, several researchers have already considered glass-fiber reinforced composites as a potential material in VIPV applications [12,17-19]. In previous studies [19,21], it was found that LW modules based on non-reinforced polymer materials and conventional tabbing and stringing connection technology suffered busbar-ribbon disconnection through thermal cycling. In this work, we present the first LW module architecture using a commercially available carbon-fiber reinforced polypropylene (CFPP) and different multiwire designs, aiming for increased aesthetics for VIPV. Following the thermal cycling test based on IEC 61215:2021[22], we demonstrate that CFPP modules are more reliable in the thermal cycling test due to better (thermo-)mechanical properties of a CFPP compared to a glass-fiber reinforced polypropylene (GFPP) backsheet. Adapting polymer encapsulant and interconnection foil to glass-fiber reinforcement materials is implemented to improve thermo-mechanical reliability. Significant thermal stresses induced failures in wire interconnects are observed by electroluminescence (EL) and X-ray-based micro-tomography (µ-CT) images. Therefore, this work could potentially contribute to the application of additional research methods in investigating the reliability of LW modules made from commercially available composite materials. It can also provide guidelines for LW PV module design, and the research could shed light on the potential of LW PV modules specifically for VIPV applications.

II. EXPERIMENTAL SECTION

2.1. Module fabrication

Figure 1 (a) shows the schematic build-up of LW mini-modules (2x1 cells. The LW PV modules have three essential compositions: the fiber-reinforced polymer backsheet, cell string interconnects, and a polymer frontsheet, which are encapsulated by a commercial polyolefin (PO) using a membrane laminator under 700 mbar at 165 °C for 24 minutes. The composite backsheet is fabricated with a unidirectional GFPP or CFPP tape in an $[0/90]_s$ configuration, as seen in Figure 1 (b), at 175 °C under 1000 mbar for 10 minutes, following a controlled cooling step with max. 7.5°C/min until reaching room temperature. Silicon heterojunction cell strings are interconnected by multiwire interconnection technology, which is composed of 18 copper interconnection wires in a core diameter of 250 µm coated with an 8 µm thick SnBiAg coating as interconnects and a PO as a carrier foil (marked as MW1). The carrier foil was modified to improve thermomechanical reliability by adding 10% short glass fiber (details described in the patent [24], marked as MW2). Three mini-modules were fabricated for each configuration in the following tests.

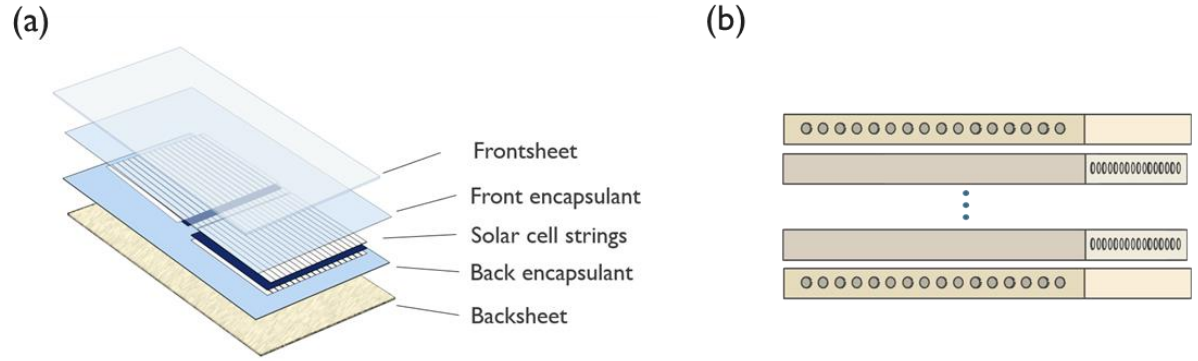

Figure 1. (a) The schematic build-up of a LW mini-modules (2x1 cells). (b) The structure of fiber reinforced polymer backsheet.

2.2. Accelerated aging and mechanical reliability test

Based on the IEC 61215:2021, the thermal cycling tests (- 40 to 85 °C, 3 hours, at least 200 thermal cycles) were conducted to determine the thermo-mechanical stability of LW modules. A high-temperature thermal cycling test (- 40 to 110 °C, 3.5 hours) was performed to investigate the thermomechanical stability in a harsher environment regarding VIPV applications with accelerated degradation rates (profile shown in Supportive Information Figure S1).

2.3. Structural characterization

Thermal mechanical analysis (TMA): the TMA test was carried out on a TMA Q400 machine in the temperature range from -40 to 100 °C at a rate of 3 °C/min. The coefficient of thermal expansion (CTE) of GFPP-/CFPP samples was obtained by extracting the slope of the deformation-temperature curve. Tensile tests were performed on a hydraulic Instron 3365 universal test device with a 250 N load cell at a constant strain rate of 0.01 /min for encapsulants according to ASTM D638 [25]. Five samples were produced for each test with a size of 150 mm × 13 mm (length × width). The µ-CT is based on 1800 X-ray projections obtained with a Yxlon Cheetah Evo system at 80 kV. Siemens Cera software was used for the reconstruction and rendering process. Current-voltage (IV) measurement was performed by using the

Wavelabs system, a LED-based solar simulator, and EL images were captured by a CCD detector in an MBJ system.

III. RESULTS AND DISCUSSION

3.1. Thermomechanical reliability

The thermo-mechanical reliability is firstly investigated based on the GFPP-backsheet modules using two MW foils (MW1 and MW2). Figure 2 (a) shows that, by changing the MW1 to MW2, the GFPP modules have a prominently lower FF-degradation from 48.6 % to less than 13.3 % after 200 thermal cycles. The FF degradation through the thermal cycling test mainly results from increased ohmic losses. As shown in Figure 2 (b), the series resistance of GFPP+MW1 module rises to 78.7 mΩ, which is significantly higher than that of GFPP+MW2 module (20.5 mΩ). The increased reliability of modules with MW2 is attributed to the glass fiber diminishing CTE mismatch of the material stack, thereby introducing fewer thermal stresses in the wire interconnects [26, 27]. Degradation (or failure) mechanisms will be further discussed in section 3.2.

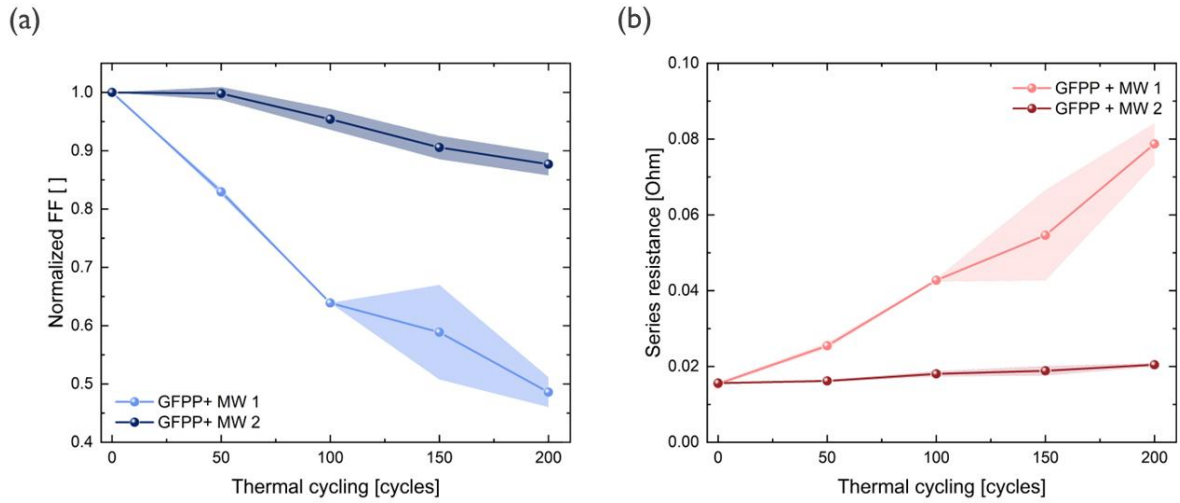

Figure 2. (a) The normalized FF and (b) the series resistance increase of GFPP modules with MW 1 and MW 2 foils through the thermal cycling test. The fast degradation of GFPP+MW1 results from a significant series resistance increase.

The (thermo-)mechanical properties of a backsheet was also found to be of significance by a numerical modelling [23] and might considerably influence the performance of lightweight modules. To find out the effect of the backsheet material selection, we implemented a CFPP-backsheet in an identical module structure with the same multiwire foils. As displayed in Figure 3 (a), modules with the CFPP-backsheet configuration have a significant increase in thermomechanical reliability compared to GFPP modules, showing the FF degradation of 30.2 % for CFPP+MW1 and 5.4 % for CFPP+MW2. As observed from Figure 3 (b), although the series resistance increase of MW 1 is considerably modulated by using the CFPP backsheet compared to GFPP modules, CFPP modules with MW 2 demonstrate less increase in series resistance. To further elaborate the understanding of backsheet effect, we performed the TMA test on the GFPP and CFPP-backsheet samples to measure their CTE, as shown in Figure S2 (fitting parameters listed in SI Table S1). We find that the CTE of CFPP (3.6×10^{-6}/K) is remarkably lower than the CTE of GFPP (58-164 $\times10^{-6}$/K) with a good correlation from previous studies, which suggested the CTE of a frontsheet or backsheet should be in the range of CTE of copper and Si to resist thermal stresses [23]. Interestingly, the CTE of CFPP is comparable to that of a soda-lime glass used in the PV industry (CTE of glass ~ 9 $\times10^{-6}$/K). Thus, CFPP can be identified as an essentially “thermo-stiff” layer in the LW structure, having

a global impact to remain the module morphology of the module and leading to less deformation over the module through the thermal cycling test, which can be beneficial to constrain thermal stresses.

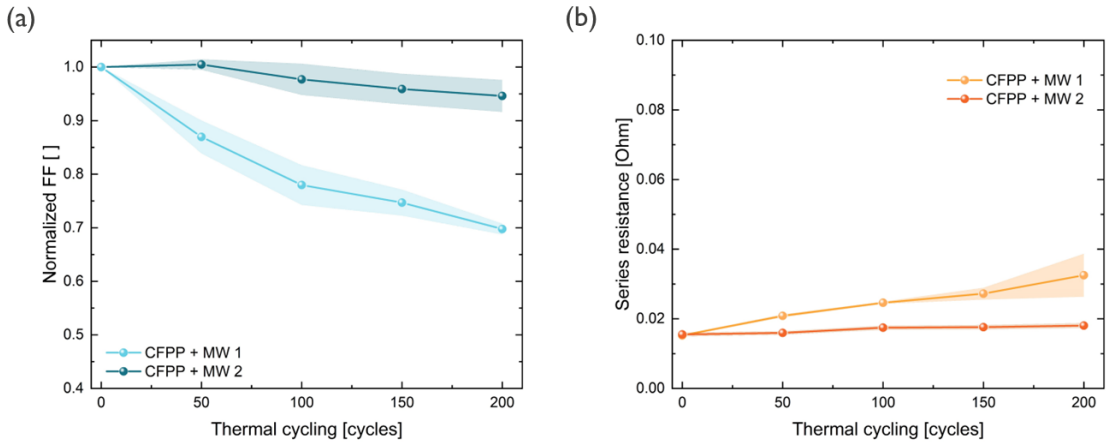

Figure 3. (a) The normalized FF and (b) the series resistance increase of CFPP modules with MW 1 and MW 2 foils through the thermal cycling test.

The use of CFPP-backsheet in the LW module can lead to thermomechanical reliability of the module approaching to a 5 % FF loss after 200 thermal cycles, yet not sufficient to pass the thermal cycling test regulated in IEC 61215. Next, we deployed a randomly chopped short glass-fiber sheet to reinforce the back encapsulant (in a 10 % weight ratio), which improves the reliability of CFPP-module with an FF loss of only 2.9 % and a low deviation after 200 thermal cycles, as seen in Figure 4. According to a previously reported study [20], the increased reliability could be ascribed to a reduced CTE. Moreover, we notice that the stiffness of the encapsulant is remarkably boosted by adding the GF into polymer with a complete change of the encapsulant from a polymer to a brittle composite, which increases the E modulus from 19.05 MPa to 343.28 MPa at room temperature, as tensile test results illustrated in Figure S3, showing that the high E modulus brings more coupling between cell strings and backsheet [23]. The results highlight the significance of adding glass fiber into the LW module architecture, not only in decreasing the CTE, but also increasing the stiffness of the back encapsulant to reach a higher correlation with the backsheet.

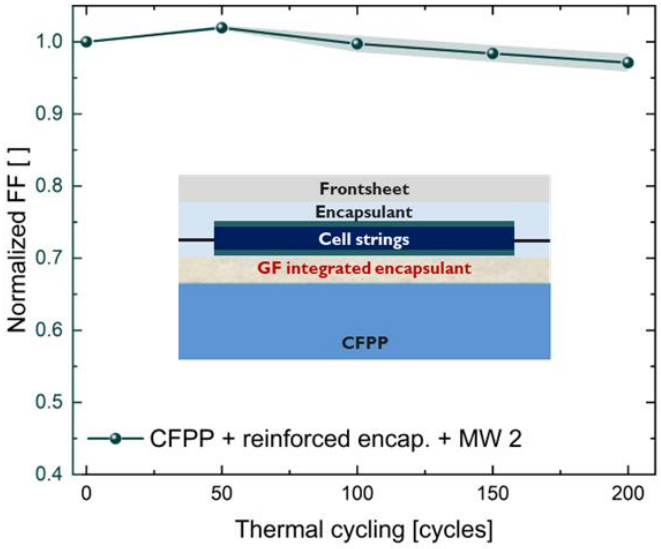

Figure 4. The normalized FF of modules with the CFPP backsheet, glass fiber reinforced back encapsulant (10% in weight ratio), and MW2 foil. The structure shows a favourable thermo-mechanical reliability with the FF decrease of only 2.9 % after 200 cycles.

3.2. Failure mechanism analysis

Furthermore, to understand the failure mechanisms in the LW modules, we performed EL imaging on both GFPP and CFPP modules. The EL images imply weak connections between wire and finger metallization at the cell edges and in-between solar cells (Figure 5) in all modules. However, modules with MW 1 demonstrate more severe disconnections. Considering such a configuration does not contain any glass fiber in interconnection foil and encapsulant, materials (in the module stack) will expand or shrink during the temperature change due to the larger CTE differences. This leads to the highest stresses along the edges of the cells at the extremities of wires, confirmed by the prior numerical simulation [28]. These high stresses, particularly at the edges, cause mechanical disconnection of contacts, while changing MW foil and backsheet (MW1 to MW2 and GFPP to CFPP) can limit thermo-mechanical stress as discussed in 3.1.

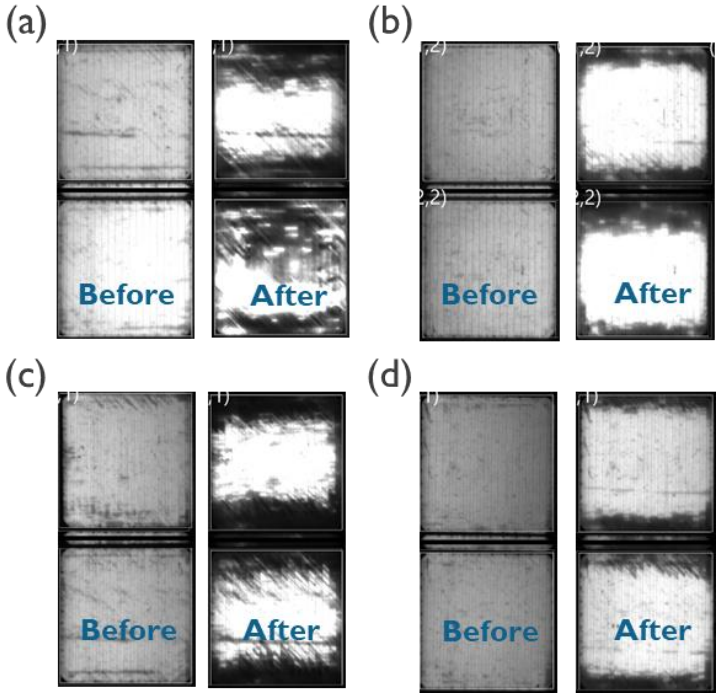

Figure 5. EL pictures of LW modules with a structure of (a) GFPP-MW1 (b) GFPP-MW2 (c) CFPP-MW1 (d) CFPP-MW2 before and after the TC test.

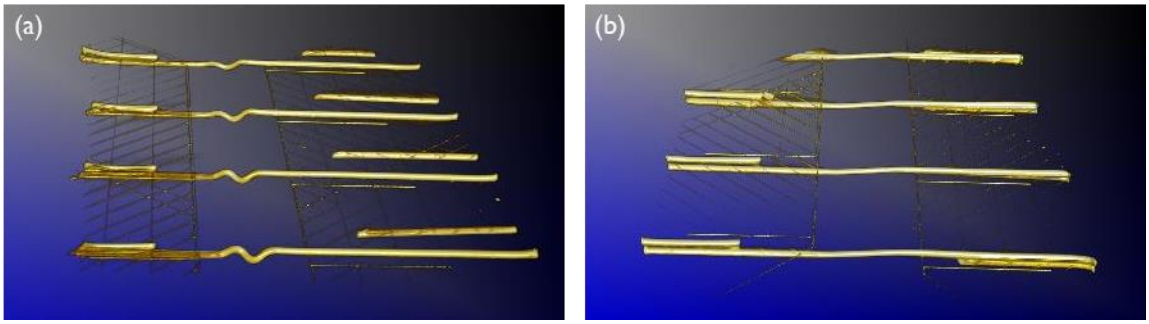

Figure 6. Rendered µ-CT images of (a) GFPP-MW1 and (b) CFPP-MW 1 modules after the TC test.

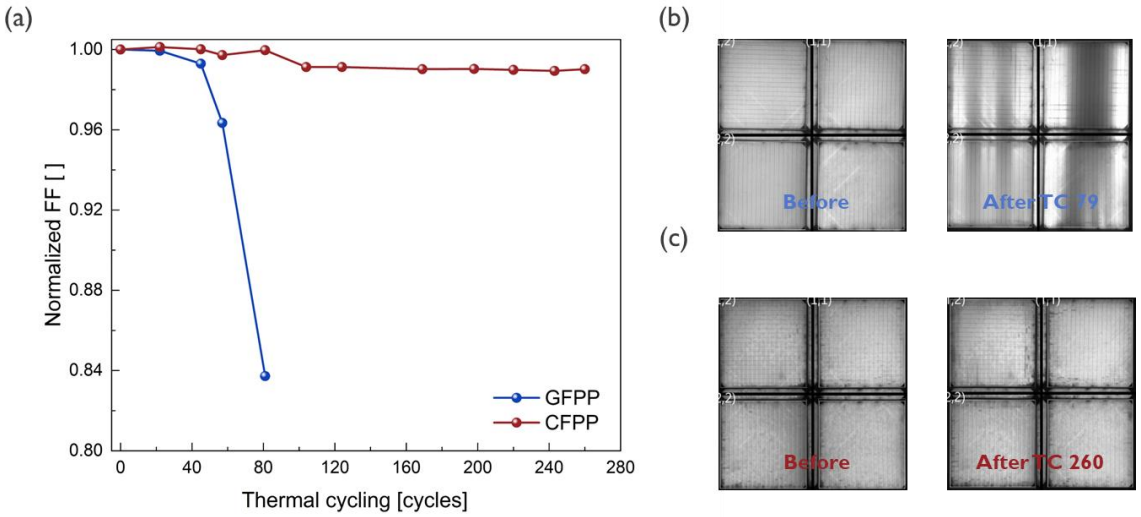

Figure 7. (a) The normalized FF of GFPP and CFPP modules through high-temperature thermal cycling test (b) EL images of GFPP modules before and after 79 high temperature thermal cycles (c) EL images of CFPP modules before and after 260 thermal cycles

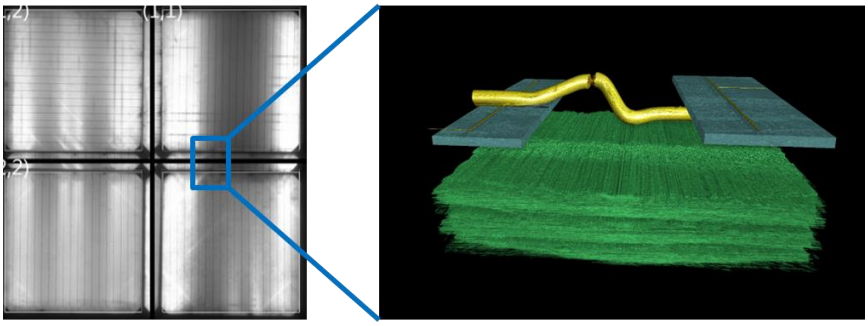

Figure 8. The EL image of the GFPP module after 79 high-temperature thermal cycles (left) points out that the focus area in the rendered µ-CT image in the GFPP module focuses on the in-between solar cell interconnects, which shows a clear breakage of wire through the thermal cycling test (right).

Coming back to Figures 2 (b) and 3 (b), the increased series resistance is aligned with a reduced contact area between cell metallization and wire interconnects indicated by EL imaging. Series resistance increase is a common degradation mode after thermal cycling test [29-31], which suggests the lost contacts of wire and cell metallization through the test due to CTE mismatch of wire interconnects and Si. After taking a closer look at the area in-between two solar cells by µ-CT, interestingly, we find the wires are vertically twisted especially in GFPP modules, as presented in Figure 6 (a). This can be interpreted to the effect of thermal stress and strain compressing and deforming the wires between the cells through the thermal cycling test due to a relatively large CTE of polymer materials and vertical CTE mismatch that gives a vertical deformation. However, when looking at the CFPP module, the interconnect wires are hardly twisted, as shown in Figure 6 (b). This can be explained by the extremely low CTE of the CFPP backsheet as discussed previously. To figure out if reinforced encapsulant can mitigate the effect of twist wires in GFPP configuration, we also produced GFPP modules with MW2 and using reinforced encapsulant (adding GF into back encapsulant); nevertheless, we find that even if the implementation of the reinforced encapsulant cannot mitigate the effect of twisted wires (see the µ-CT image in Figure S4). This observation might suggest the importance of using a "thermal-stiff" layer as backsheet in the LW module structure. The twisted wire might, on the one hand, act as a buffer to compensate for the further thermal expansion or shrinkage of wires in the horizontal direction; on the other hand, it may lead to fatigue stress in interconnects. To determine the effects of twisted wires, in the following experiment, we artificially deformed commercial multiwire interconnect foils in the interconnection area between the cells in a cell string and produced GFPP and CFPP modules with identical architecture. Considering our aim was to adapt this LW module with a multiwire design into VIPV applications, we conducted an adapted high-temperature thermal cycling test (- 40 to 110 °C, 3.5 h), since the surface temperature for automotive during parking could be significantly higher than 85 °C, potentially causing enormous degradation and unexpected failures [14]. Figure 7 (a) demonstrates the FF degradation of GFPP and CFPP modules. Interestingly, the GFPP module shows a large drop in performance after 79 cycles. The EL image of the GFPP module in Figure 7 (b) indicates the disconnection in between cells. We, again, use µ-CT to detect the interconnects in-between two cells and observe wire disruptions as illustrated in Figure 8, which could be explained by significantly concentrated thermal stresses (also supported by the reported study [21]) that account for tremendous fatigue stresses. Although the CFPP module was fabricated with a twisted foil as well, it still has a favorable reliability with only ~ 3 % performance loss and minor degradation from the EL image (as shown in Figure 7 c) after 260 thermal cycles due to the implementation of the CFPP backsheet. The outcomes from the high-temperature thermal cycling test further support the beneficial effect on the reliability of LW modules when using CFPP and multiwire design in VIPV applications.

IV. CONCLUSION AND OUTLOOK

In this paper, we present a comprehensive thermo-mechanical reliability assessment of lightweight modules with a structure using a commercial fiber-reinforced, composite backsheet and a multiwire design, especially targeting VIPV applications. Modules fabricated with a purely polymeric multiwire foil and a GFPP backsheet can have significant performance losses over 200 thermal cycles, while modules with glass fiber integrated polymers (including MW foil and encapsulant) and CFPP modules demonstrate a preferable thermo-mechanical reliability showing the FF decrease of only 2.9 %. The use of composite encapsulant can reduce the CTE differences in material stack and establish a favorable coupling between solar cell strings and backsheet due to a dramatically increased stiffness (E modulus). Therefore, the implementation of a composite encapsulant and low CTE backsheet (CFPP) is beneficial to thermo-mechanical reliability.

The primary failure mechanism is visualized by EL and µ-CT, which is identified as electrical disconnection of wire and cell metallization at the edges of cells as well as wire breakage in-between cells, where the thermal stresses are concentrated through thermal cycles. The thermal expansion and compression of materials in the module stack introduces twisted wires especially in GFPP modules due to a large CTE mismatch of the materials in the module stack, which leads to fatigue stresses concentration in-between solar cells during thermal cycling tests, causing wire breakage in a fast degradation reliability test, namely high-temperature thermal cycling test (-40 to 110 °C, 3.5 h). The findings of this work suggest that a backsheet with a low CTE such as CFPP is required for glass-free VIPV modules in order to avoid the effect of thermal stress concentration causing interconnection failure, which is indicative of further improvement of lightweight PV modules for VIPV applications, considering higher requirements in lightweight, aesthetics and reliability aspects.

ACKNOWLEDGEMENT

The authors gratefully acknowledge the Flemish government for its financial support through the funded ICON projects SNRoof and related project partners, as well as the European Union's Horizon 2020 Programme for research, technological development and demonstration for funding part of this work under Grant Agreement no. 857793. The authors also would like to acknowledge the partial funding by the Kuwait Foundation for the advancement of Sciences under project number P115-15EE-01.

CONFLICT OF INTEREST

The authors declare no conflict of interest.

DATA AVAILABILITY STATEMENT

The data that support the findings of this study are available from the corresponding authors upon reasonable request.

AUTHOR CONTRIBUTIONS

B. Luo, J. Govaerts, R. V. Dyck, T. Borgers conceived the idea and planned experiments. B. Luo coordinated the work and conducted module fabrication, IV and EL measurements, analyzed results and prepared manuscript as well as figures. B. Ruttens and J. D'Haen

conducted μ-CT. R. V. Dyck conducted TMA for GFPP and CFPP materials. B.Luo and M. Paesa carried out the tensile test. M. J. Govaerts, L. Tous, H. S. Radhakrishnan, M. Daenen, A. Van Vuure and J. Poortmans contributed conceptual ideas, results interpretation and supervised the work. All authors made valuable comments and contributed to manuscript.

REFERENCE

[1] A. Dik, S. Omer, and R. Boukhanouf, "Electric Vehicles: V2G for Rapid, Safe, and Green EV Penetration," *Energies*, vol. 15, no. 3, Art. no. 3, Jan. 2022, doi: 10.3390/en15030803.

[2] "Market monitor: European passenger car and light commercial vehicle registrations, January–December 2021," *International Council on Clean Transportation*. https://theicct.org/publication/market-monitor-eu-jan-to-dec-feb22/ (accessed Jan. 29, 2023).

[3] M. Heinrich, D. H. Neuhaus, L. E. Alanis, and C. Kutter, "Yield Potential of Vehicle Integrated Photovoltaics on Commercial Trucks and Vans," *38th Eur. Photovolt. Sol. Energy Conf. Exhib.*, pp. 1412–1420, Nov. 2021, doi: 10.4229/EUPVSEC20212021-6DO.8.2.

[4] Y. Ota, K. Araki, A. Nagaoka, and K. Nishioka, "Facilitating vehicle-integrated photovoltaics by considering the radius of curvature of the roof surface for solar cell coverage," *Clean. Eng. Technol.*, vol. 7, p. 100446, Apr. 2022, doi: 10.1016/j.clet.2022.100446.

[5] M. Yamaguchi *et al.*, "Analysis for the Potential of High-Efficiency and Low-Cost Vehicle-Integrated Photovoltaics," *Sol. RRL*, vol. n/a, no. n/a, p. 2200556, doi: 10.1002/solr.202200556.

[6] C. Thiel *et al.*, "Impact of climatic conditions on prospects for integrated photovoltaics in electric vehicles," *Renew. Sustain. Energy Rev.*, vol. 158, p. 112109, Apr. 2022, doi: 10.1016/j.rser.2022.112109.

[7] O. Kanz, A. Reinders, J. May, and K. Ding, "Environmental Impacts of Integrated Photovoltaic Modules in Light Utility Electric Vehicles," *Energies*, vol. 13, no. 19, Art. no. 19, Jan. 2020, doi: 10.3390/en13195120.

[8] "State of the Art & Expected Benefits of PV-Powered Vehicles," *IEA-PVPS*. https://iea-pvps.org/key-topics/state-of-the-art-and-expected-benefits-of-pv-powered-vehicles/ (accessed Jan. 29, 2023).

[9] R. Peibst *et al.*, "Demonstration of Feeding Vehicle-Integrated Photovoltaic-Converted Energy into the High-Voltage On-Board Network of Practical Light Commercial Vehicles for Range Extension," *Sol. RRL*, vol. 6, no. 5, p. 2100516, 2022, doi: 10.1002/solr.202100516.

[10] A. C. Martins, V. Chapuis, F. Sculati-Meillaud, A. Virtuani, and C. Ballif, "Light and durable: Composite structures for building-integrated photovoltaic modules," *Prog. Photovolt. Res. Appl.*, vol. 26, no. 9, pp. 718–729, 2018, doi: 10.1002/pip.3009.

[11] A. C. Martins, V. Chapuis, A. Virtuani, and C. Ballif, "Ultra-Lightweight PV module design for Building Integrated Photovoltaics," in *2017 IEEE 44th Photovoltaic Specialist Conference (PVSC)*, Jun. 2017, pp. 2104–2108. doi: 10.1109/PVSC.2017.8366791.

[12] A. C. Martins, V. Chapuis, A. Virtuani, and C. Ballif, "Robust Glass-Free Lightweight Photovoltaic Modules With Improved Resistance to Mechanical Loads and Impact," *IEEE J. Photovolt.*, vol. 9, no. 1, pp. 245–251, Jan. 2019, doi: 10.1109/JPHOTOV.2018.2876934.

[13] F. Lisco, A. C. Martins, A. Virtuani, and C. Ballif, "Glass-Free Lightweight Solar Modules for Integrated Photovoltaics: The Use of Velcro as an Alternative Mounting System," in *Proceedings of the 37th European Photovoltaic Solar Energy Conference and Exhibition, Lisbon, Portugal*, 2020, pp. 7–11.

[14] J. Markert, C. Kutter, B. Newman, P. Gebhardt, and M. Heinrich, “Proposal for a Safety Qualification Program for Vehicle-Integrated PV Modules,” *Sustainability*, vol. 13, no. 23, Art. no. 23, Jan. 2021, doi: 10.3390/su132313341.
[15] U. E. Secretariat, “Agreement concerning the Adoption of Uniform Technical Prescriptions for Wheeled Vehicles, Equipment and Parts Which Can Be Fitted and/or Be Used on Wheeled Vehicles and the Conditions for Reciprocal Recognition of Approvals Granted on the Basis of These Prescriptions :,” Feb. 2002, Accessed: Jan. 29, 2023. [Online]. Available: https://digitallibrary.un.org/record/459783
[16] S. Kim, M. Holz, S. Park, Y. Yoon, E. Cho, and J. Yi, “Future Options for Lightweight Photovoltaic Modules in Electrical Passenger Cars,” *Sustainability*, vol. 13, no. 5, Art. no. 5, Jan. 2021, doi: 10.3390/su13052532.
[17] P. K. Mallick, “2 - Advanced materials for automotive applications: an overview,” in *Advanced Materials in Automotive Engineering*, J. Rowe, Ed. Woodhead Publishing, 2012, pp. 5–27. doi: 10.1533/9780857095466.5.
[18] J. Govaerts *et al.*, “The Potential of Glass-Fibre-Reinforcement: (Thermo-)Mechanical Testing of Light-Weight PV Modules,” *38th Eur. Photovolt. Sol. Energy Conf. Exhib.*, pp. 24–27, Nov. 2021, doi: 10.4229/EUPVSEC20212021-1AO.3.1.
[19] J. Govaerts *et al.*, “On the Road towards Vehicle Integration: Glass-Fibre Reinforced Encapsulation Enabling Light-Weight and Curved Modules,” *37th Eur. Photovolt. Sol. Energy Conf. Exhib.*, pp. 98–102, Oct. 2020, doi: 10.4229/EUPVSEC20202020-1BV.4.47.
[20] J. Govaerts *et al.*, “Development and testing of light-weight PV modules based on glass-fibre reinforcement,” *EPJ Photovolt.*, vol. 13, p. 13, 2022, doi: 10.1051/epjpv/2022007.
[21] D. H. Neuhaus, M. Heinrich, J. Markert, L. E. Alanis, F. Basler, and C. Kutter, “Integrated Lightweight, Glass-Free PV Module Technology for Box Bodies of Commercial Trucks,” *37th Eur. Photovolt. Sol. Energy Conf. Exhib.*, pp. 1711–1718, Oct. 2020, doi: 10.4229/EUPVSEC20202020-6DO.11.6.
[22] “IEC 61215-2:2021 | IEC Webstore.” https://webstore.iec.ch/publication/61350 (accessed Jan. 29, 2023).
[23] A. J. Beinert, P. Romer, M. Heinrich, J. Aktaa, and H. Neuhaus, “Thermomechanical design rules for photovoltaic modules,” *Prog. Photovolt. Res. Appl.*, vol. n/a, no. n/a, doi: 10.1002/pip.3624.
[24] T. Borgers and J. Govaerts, “Methods for electrically contacting and interconnecting photovoltaic cells,” EP3790059A1, Mar. 10, 2021 Accessed: Jan. 31, 2023. [Online]. Available: https://patents.google.com/patent/EP3790059A1/en
[25] “Standard Test Method for Tensile Properties of Plastics.” https://www.astm.org/d0638-22.html (accessed Jan. 29, 2023).
[26] J. Poortmans *et al.*, “The Beauty as well as the Beast: Towards Appealing Aesthetics and Reliable Photovoltaics for Vehicle Integration and Beyond,” *8th World Conf. Photovolt. Energy Convers.*, pp. 562–565, Dec. 2022, doi: 10.4229/WCPEC-82022-3CO.5.3.
[27] R. Van Dyck, T. Borgers, J. Govaerts, J. Poortmans, and A. W. van Vuure, “Three-dimensional multi-ribbon interconnection for back-contact solar cells,” *Prog. Photovolt. Res. Appl.*, vol. 29, no. 5, pp. 507–515, 2021, doi: 10.1002/pip.3390.
[28] G. Li *et al.*, “Thermo-mechanical behavior assessment of smart wire connected and busbarPV modules during production, transportation, and subsequent field loading stages,” *Energy*, vol. 168, pp. 931–945, Feb. 2019, doi: 10.1016/j.energy.2018.12.002.
[29] M. T. Zarmai, N. N. Ekere, C. F. Oduoza, and E. H. Amalu, “A review of interconnection technologies for improved crystalline silicon solar cell photovoltaic module assembly,” Applied Energy, vol. 154, pp. 173–182, Sep. 2015, doi: 10.1016/j.apenergy.2015.04.120. (accessed Feb. 22, 2023).

[30] Y. Du, L. Wang, and W. Tao, “Modeling, imaging and resistance analysis for crystalline silicon photovoltaic modules failure on thermal cycle test,” Engineering Failure Analysis, vol. 118, p. 104818, Dec. 2020, doi: 10.1016/j.engfailanal.2020.104818.
[31] C. Radue and E. E. van Dyk, “A comparison of degradation in three amorphous silicon PV module technologies,” Sol. Energy Mater. Sol. Cells, vol. 94, no. 3, pp. 617–622, Mar. 2010, doi: 10.1016/j.solmat.2009.12.009.

Supplementary Information

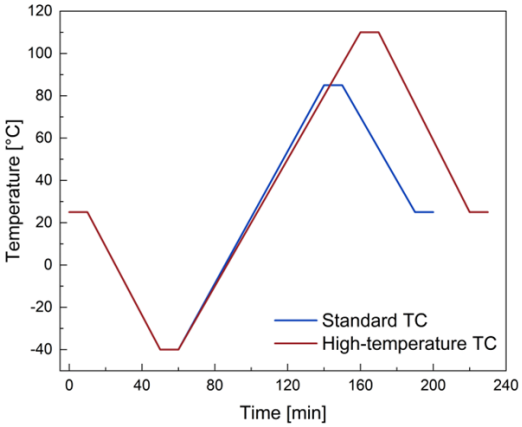

Figure S1. The profile of standard thermal cycling test () and adapted high-temperature thermal cycling test ()

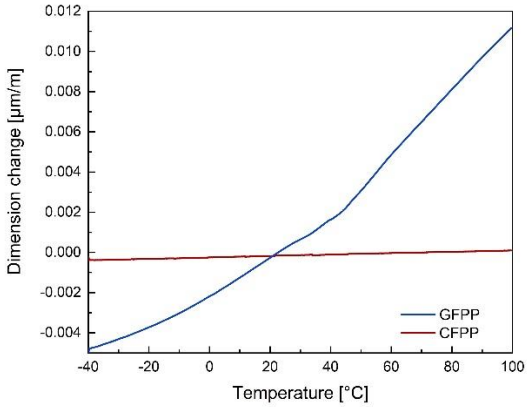

Figure S2. The profile of standard thermal cycling test and adapted high-temperature thermal cycling test

Table S1. Fitting parameters of GFPP and CFPP

Name	CTE (α) [10^{-6} / °C]
GFPP (-40 to 40 °C)	58.0
GFPP (40 to 100 °C)	164.2
CFPP	3.6

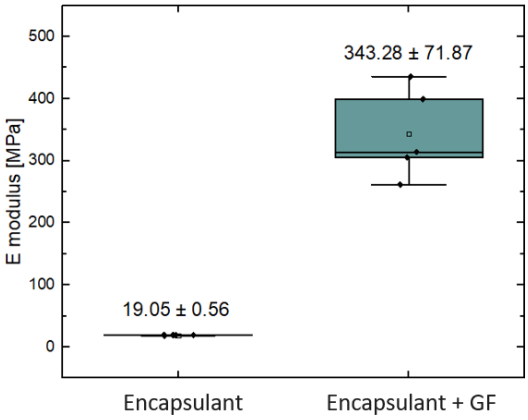

Figure S3. The E modulus of encapsulant and reinforced encapsulant (marked as encapsulant + GF).

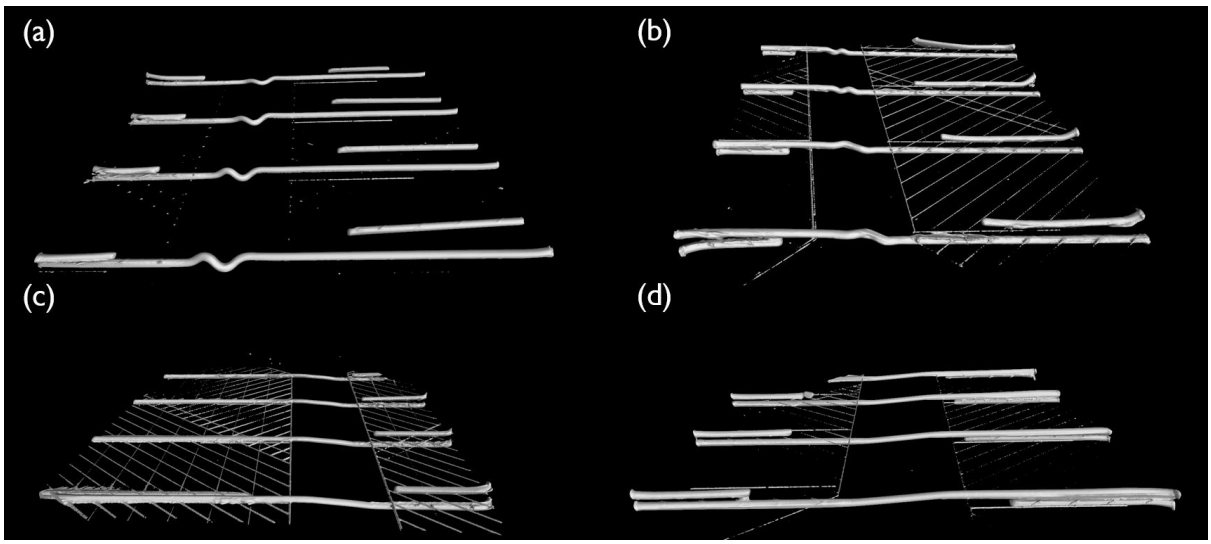

Figure S4. Rendered µ-CT images of (a) GFPP-MW1, (b) GFPP-GF-MW2, (c) CFPP-GF-MW 2 and (d) CFPP-MW 1 modules after the TC test. (a) and (b) illustrate the wire deformation in all modules with GFPP backsheet with or without GF integrated in back encapsulant, while (c) and (d) hardly show any wire deformation.